

Introducing high-throughput sequencing into mainstream genetic diagnosis practice in inherited platelet disorders

José M. Bastida,^{1,3} María L. Lozano,^{2,3} Rocío Benito,⁴ Kamila Janusz,⁴ Verónica Palma-Barqueros,² Mónica Del Rey,⁴ Jesús M. Hernández-Sánchez,⁴ Susana Riesco,⁵ Nuria Bermejo,⁶ Hermenegildo González-García,⁷ Agustín Rodríguez-Alén,⁸ Carlos Aguilar,⁹ Teresa Sevivas,¹⁰ María F. López-Fernández,¹¹ Anna E. Marneth,¹² Bert A. van der Reijden,¹² Neil V. Morgan,¹³ Steve P. Watson,¹³ Vicente Vicente,³ Jesús M. Hernández-Rivas,^{1,4} José Rivera^{*2,3} and José R. González-Porras^{*1}

¹Servicio de Hematología, Hospital Universitario de Salamanca-IBSAL-USAL, Spain; ²Servicio de Hematología y Oncología Médica, Hospital Universitario Morales Meseguer, Centro Regional de Hemodonación, Universidad de Murcia, IMIB-Arrixaca, CB15/00055-CIBERER, Spain; ³On behalf of the Project “Functional and Molecular Characterization of Patients with Inherited Platelet Disorders” of the Hemorrhagic Diathesis Working Group of the Spanish Society of Thrombosis and Haemostasis; ⁴IBSAL, IBMCC, CIC, Universidad de Salamanca-CSIC, Spain; ⁵Servicio de Pediatría, Hospital Universitario de Salamanca-IBSAL, Spain; ⁶Servicio de Hematología, Complejo Hospitalario San Pedro Alcántara, Cáceres, Spain; ⁷Servicio de Pediatría, Hospital Clínico Universitario de Valladolid, Spain; ⁸Servicio de Hematología y Hemoterapia, Hospital Virgen de la Salud, Complejo Hospitalario de Toledo, Spain; ⁹Servicio de Hematología, Complejo Asistencial de Soria, Spain; ¹⁰Serviço de Imunohemoterapia, Sangue e Medicina Transfusional do Centro Hospitalar e Universitário de Coimbra, EPE, Portugal; ¹¹Servicio Hematología y Hemoterapia, Complejo Hospitalario Universitario A Coruña, Spain; ¹²Department of Laboratory Medicine, Laboratory of Hematology, Radboud Institute for Molecular Life Sciences, Radboud University Medical Centre, Nijmegen, the Netherlands and ¹³Birmingham Platelet Group, Institute of Cardiovascular Sciences, College of Medical and Dental Sciences, University of Birmingham, UK

**JR and JRG-P contributed equally to this work*

©2017 Ferrata Storti Foundation. This is an open-access paper. doi:10.3324/haematol.2017.171132

Received: April 20, 2017.

Accepted: September 29, 2017.

Pre-published: October 5, 2017.

Correspondence: jmbastida@saludcastillayleon.es / jose.rivera@carm.es

Introducing high-throughput sequencing into mainstream of genetic diagnosis practice in inherited platelet disorders.

Bastida et al.

Supplemental Methods

Blood sampling, platelet phenotyping and DNA isolation

Venous blood was drawn from each patient into commercial 7.5% K3 EDTA tubes (for complete blood count [CBC], and DNA isolation), and into buffered 3.2% sodium citrate for platelet studies. Platelet function testing was performed mainly in citrated platelet-rich-plasma. Assays included, as appropriate, blood smears, PFA-100, light transmission aggregometry, flow cytometric evaluation of platelet glycoprotein's and agonist-induced platelet activation, alpha and dense granule secretion, clot retraction, immunoblotting analysis of selected proteins, immunofluorescence and electron microscopy.¹⁻³ Genomic DNA from peripheral blood samples was isolated using a DNeasy blood and tissue kit, following the manufacturer's protocol (Qiagen, Hilden, Germany). DNA concentration was measured using a Qubit 2.0 fluorometer (Life Technologies, Carlsbad, CA).

High-throughput sequencing (HTS)

The HTS test was performed on a MiSeq Instrument, running MiSeq Control Software and applying a Nextera sequencing design (Illumina). Fifty ng of patient's DNA was sequenced following Illumina's standardized protocol. DNA libraries were normalized to 4 nM and pooled in equal volumes. We used the 300-cycle reagent kit. Specifically, samples were sequenced using paired 150 nt reads, multiplexing twelve, dual-indexed samples per run. Twenty-four samples were included in each run.

Sanger sequencing

To verify candidate variants found using the HTS multigenic platform and to examine their segregation among available family members, we performed standard Sanger sequencing. Briefly, specific forward and reverse primers were designed using Primer3 (<http://bioinfo.ut.ee/primer3-0.4.0/primer3/>) (sequences available on request). Genomic DNA was amplified with the Fast Start High Fidelity PCR System (Roche, Basel,

Switzerland) following the manufacturer's instructions, with some variations in the annealing temperature. DNA sequences were evaluated using Chromas Lite v2.1.1 (Technelysium, South Brisbane, Australia) and DS Gene v1.5 (Accerlys, San Diego, CA) software. Data were analyzed using annotations of genome version hg19/GRCh37.

Supplemental Tables

Table S1. Diagnosis of inherited platelet disorder and underlying causative variants previously identified by Sanger sequencing, in the 10 patients of the validation group.

Case	Diagnosis	Gene	Status	Sanger Sequencing		Ref
				cDNA	Protein change	
1	CAMT	<i>MPL</i>	Hom	c.304C>T	p.Arg102Cys	1
2	CHS	<i>LYST</i>	Hom	c.11173G>A	p.Gly3725Arg	1
3	CHS	<i>LYST</i>	Hom	c.772T>C	p.Cys258Arg	
4	GT	<i>ITGA2B</i>	C. Het	c.2944G>A	p.Val982Met	1
				c.2965G>A	p.Ala989Thr	
				c.1612G>T	p.Glu538*	
5	GT	<i>ITGB3</i>	C. Het	c.647A>G	p.Tyr216Cys	1
				c.665T>C	p.Leu222Pro	
6	BSS	<i>GP1BA</i>	Hom	c.673T>A	p.Cys225Ser	1
7	BSS	<i>GP9</i>	Hom	c.212T>C	p.Phe71Ser	
8	BSS	<i>GP1BA</i>	Het	c.268_276del GGGACGCTG	p.Gln90_Leu92del	1
9	HPS	<i>HPS1</i>	Hom	c.610G>T	p.Glu204*	1,8
10	GPS	<i>GF11B</i>	Het	c.859C>T	p.Gln287*	9

Abbreviations: CAMT: Congenital amegakaryocytic thrombocytopenia; CHS: Chediak-Higashi Syndrome; GT: Glanzmann thrombasthenia; BSS: Bernard Soulier Syndrome, HPS: Hermansky-Pudlak Syndrome; GPS: Gray Platelet Syndrome; Hom: Homozygous; Het: Heterozygous; *: stop codon.

Table S2. Target regions in the 72-gene HTS platform covered with a depth read lower than 20X.

Genes	Region	Exon	Mean coverage
A2M	chr12:9264755-9264807	4	4,6
ABCA1	chr9:107586746-107586859	17	0
ANKRD26	chr10:27311487-27311616	29	14,6
	chr10:27313376-27313488	28	18,2
	chr10:27318215-27318285	26	4
	chr10:27333086-27333119	19	10,8
ANO6	chr12:45810482-45810687	17	0
AP3B1	chr5:77461434-77461496	12	18,6
BLOC1S6	chr15:45879642-45879723	1	2
DHCR24	chr1:55319710-55319907	7	17,3
	chr1:55349291-55349446	2	0
FERMT3	chr11:63990785-63990961	14	7,2
FLI1	chr11:128564154-128564171	1	14,3
GNAI3	chr1:110129351-110129504	7	11
GNAQ	chr9:80343430-80343583	6	3,5
HPS3	chr3:148847511-148847727	1	11,2
ITGB3	chr17:45331228-45331306	1	14,9
LYST	chr1:235938213-235938386	18	11,8
	chr1:235963620-235963686	8	0
MYH9	chr22:36715585-36715680	10	0
MYO5A	chr15:52680026-52680109	14	10,4
	chr15:52820977-52821003	1	16,9
PLCB2	chr15:40584050-40584125	24	5,2
RAB27A	chr15:55526980-55527132	3	16,9
RASGRP2	chr11:64503014-64503136	11	11,2
RUNX1	chr21:36265222-36265260	3	17,7
TBXAS1	chr7:139652350-139652487	6	0

Table S3. Genetic variants identified with the HTS platform, which we have recently reported in detail elsewhere.

Case	Clinical and biological phenotype	Gen Variants	IPD
28	Lifelong macrothrombocytopenia	<i>ABCG5</i>	Sitosterolemia ¹⁰
	Presence of stomatocytes in blood smear	c.1890delT	
	Xanthelasmas	c.914C>G	
66	Lifelong macrothrombocytopenia	<i>WAS</i>	Wiskott-Aldrich syndrome ¹¹
	Lack of response to previous ITP treatments	c.802delC	
90	Markedly reduced platelet aggregation with ADP, epinephrine and low-dose collagen	<i>RASGRP2</i>	α IIb β 3 activation defect ²
	Mildly reduced aggregation with other agonists		
	PFA-100 >300s; normal clot retraction		
	Normal expression of GPIIb/IIIa, GPIb/IX, GPIa and GPVI		
	Severely reduced fibrinogen binding with all agonists but PMA		
91	Markedly reduced platelet aggregation with ADP, epinephrine, low-dose collagen and CRP	<i>RASGRP2</i>	α IIb β 3 activation defect ¹²
	Mildly reduced aggregation with other agonists		
	PFA-100 >300s; normal clot retraction		
	Normal expression of GPIIb/IIIa, GPIb/IX, GPIa and GPVI		
	Reduced fibrinogen binding with all agonists but PMA		
92	Mildly reduced platelet secretion	<i>RASGRP2</i>	α IIb β 3 activation defect ¹²
	Markedly reduced platelet aggregation with all agonists		
	PFA-100 >300s; normal clot retraction		
	Normal expression of GPIIb/IIIa, GPIb/IX, GPIa and GPVI		
	Reduced fibrinogen binding with all agonist but PMA		
Mildly reduced platelet secretion	c.706C>T		

Supplemental References

1. Sanchez-Guiu I, Anton AI, Padilla J, et al. Functional and molecular characterization of inherited platelet disorders in the Iberian Peninsula: results from a collaborative study. *Orphanet J Rare Dis.* 2014;9:213.
2. Lozano ML, Cook A, Bastida JM, et al. Novel mutations in RASGRP2, which encodes CalDAG-GEFI, abrogate Rap1 activation, causing platelet dysfunction. *Blood.* 2016;128(9):1282-1289.
3. Navarro-Nunez L, Teruel R, Anton AI, et al. Rare homozygous status of P43 beta1-tubulin polymorphism causes alterations in platelet ultrastructure. *Thromb Haemost.* 2011;105(5):855-863.
4. Richards S, Aziz N, Bale S, et al. Standards and guidelines for the interpretation of sequence variants: a joint consensus recommendation of the American College of Medical Genetics and Genomics and the Association for Molecular Pathology. *Genet Med.* 2015;17(5):405-424.
5. Parrini E, Ramazzotti A, Dobyns WB, et al. Periventricular heterotopia: phenotypic heterogeneity and correlation with Filamin A mutations. *Brain.* 2006;129(Pt 7):1892-1906.
6. Stritt S, Nurden P, Turro E, et al. A gain-of-function variant in DIAPH1 causes dominant macrothrombocytopenia and hearing loss. *Blood.* 2016;127(23):2903-2914.
7. Feng Y, Chen D, Wang GL, Zhang VW, Wong LJ. Improved molecular diagnosis by the detection of exonic deletions with target gene capture and deep sequencing. *Genet Med.* 2015;17(2):99-107.
8. Sanchez-Guiu I, Torregrosa JM, Velasco F, et al. Hermansky-Pudlak syndrome. Overview of clinical and molecular features and case report of a new HPS-1 variant. *Hamostaseologie.* 2014;34(4):301-309.
9. Monteferrario D, Bolar NA, Marneth AE, et al. A dominant-negative GFI1B mutation in the gray platelet syndrome. *N Engl J Med.* 2014;370(3):245-253.
10. Bastida JM, Benito R, Janusz K, et al. Two novel variants of the ABCG5 gene cause xanthelasmas and macrothrombocytopenia: a brief review of hematological abnormalities of sitosterolemia. *J Thromb Haemost.* 2017;15(9):1859-1866.
11. Bastida JM, Del Rey M, Revilla N, et al. Wiskott-Aldrich syndrome in a child presenting with macrothrombocytopenia. *Platelets.* 28(4):417-420.

12. Sevivas T, Bastida JM, Paul DS, et al. Identification of two novel mutations in RASGRP2 affecting platelet CalDAG-GEFI expression and function in patients with bleeding diathesis. *Platelets*. 2017:1-4.

Supplemental Figures

Figure S1. Filtering strategy of variant called in 82 IPD patients analyzed by the HTS platform.

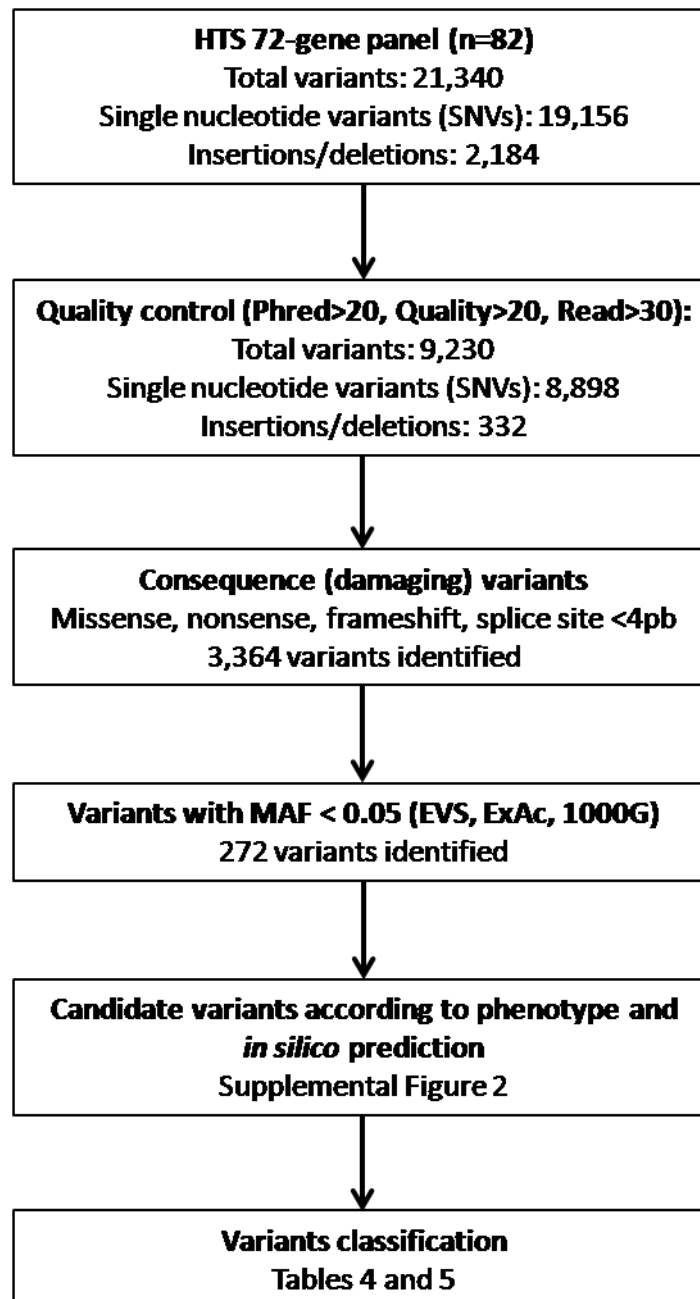


Figure S2. Gene location of variants called in each patient after the filtering procedure.

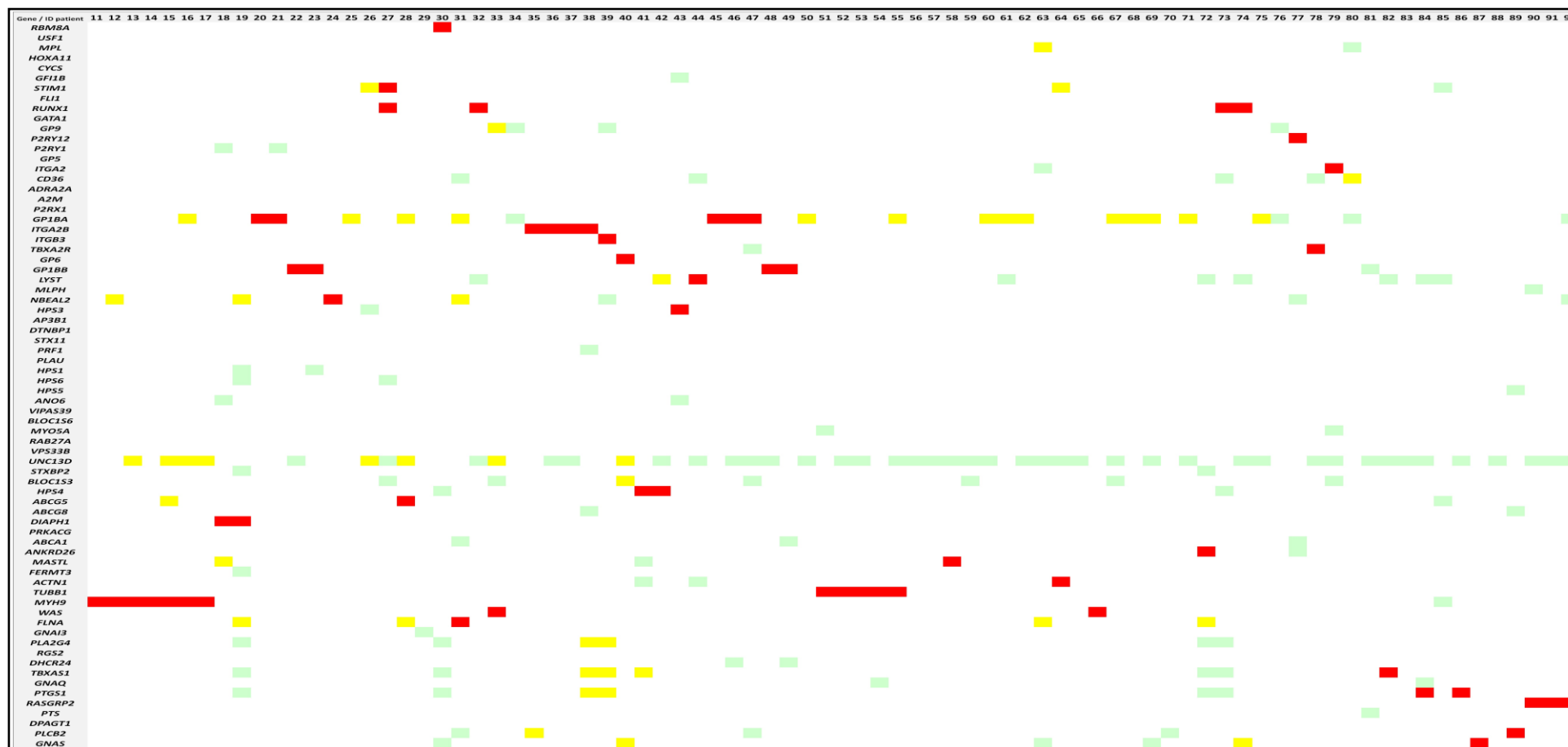


Figure S2 Legend. In each patient the filtering procedure described in Methods, led to calling one or more gene variants. These variants were qualified for contribution to the patient disease using a color code: i) Red: main candidate causal variants, which were classified for pathogenicity according to ACMG guidelines⁴; Yellow: variants in other genes that could fit with the patient phenotype (for instance, gene already known to be involved in inherited thrombocytopenia; Green: variants in other genes unknown to be involved in phenotype similar with that displayed by the patient.

Figure S3. Pedigree of the patient with c.3695C>T variant in *FLNA*.

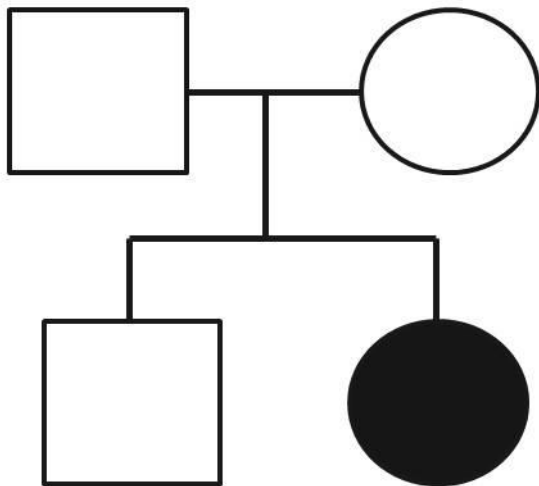


Figure S3 Legend. HTS test identified in the patient 31 (black symbol) the novel missense variant (c.3695C>T) in exon 22 of the *FLNA* gene. The patient displayed mild developmental delay and character disorders, congenital right kidney agenesis, corpus callosum hypoplasia and facial abnormalities (small mouth and eyes and bulbar nose), and moderate thrombocytopenia (40×10^9 platelets/L) [Table 2]. None of the healthy relatives (white symbols) carried this genetic variant. As occurred in our patient, variants in *FLNA* have been identified in about 20-30% of cases with sporadic bilateral periventricular nodular heterotopias.⁵

Figure S4. Family pedigrees in two unrelated families carrying the variant R1213* in *DIAPH1*.

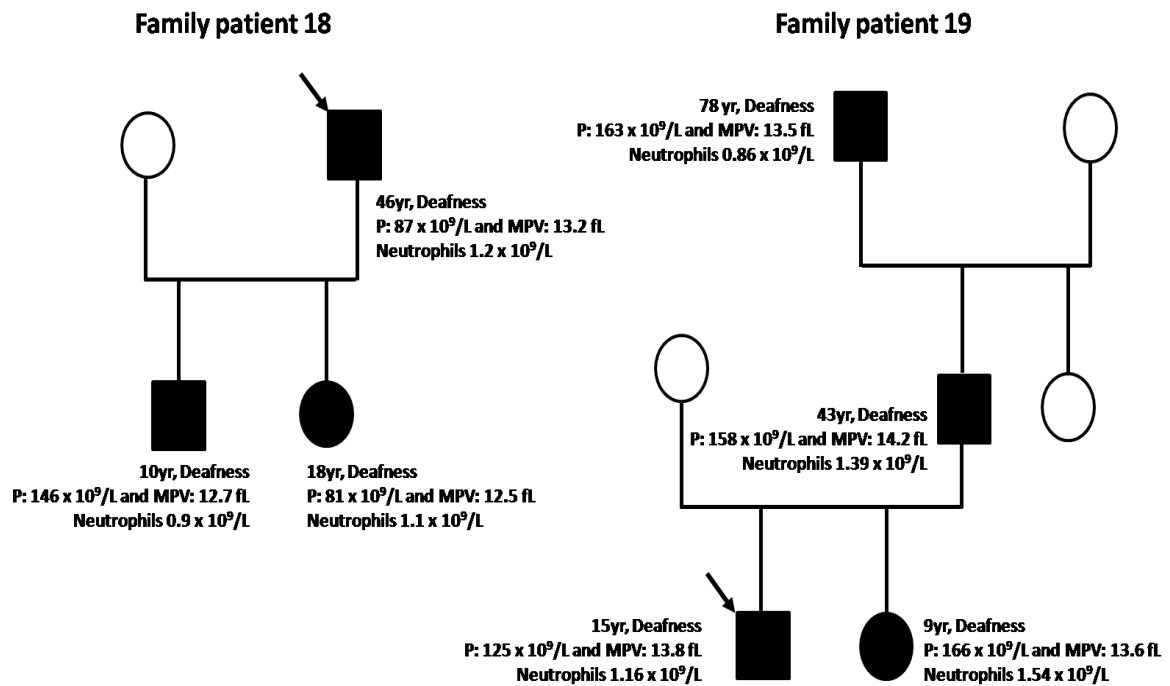


Figure S4 Legend. The index cases in each family are indicated with black arrows. Filled black symbols indicate heterozygosity for the R1213* variant in *DIAPH1*. Family members in white symbols do not carrier the R1213* variant. They showed not hearing abnormalities and displayed normal blood cell counts.

Figure S5. Platelet aggregation and secretion in carriers of the R1213* variant in *DIAPH1*.

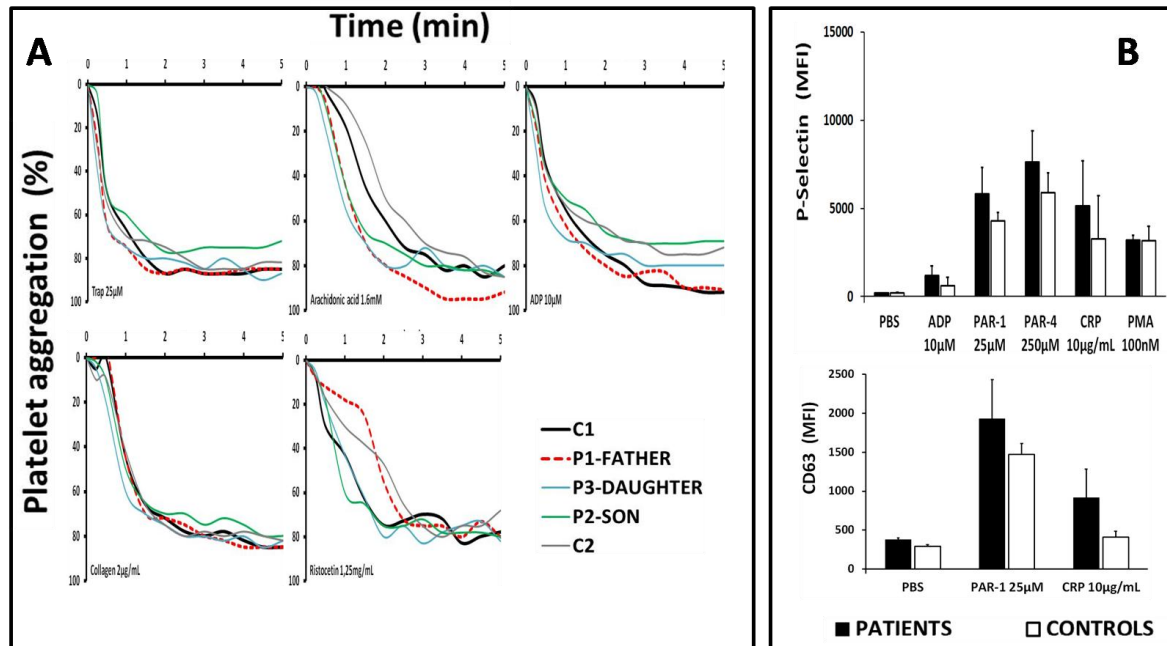


Figure S5 Legend. A) Platelet aggregation in response to the indicated platelet agonists was evaluated in unadjusted platelet-rich plasma (PRP), from patients (P1, P2, P3) and two unrelated controls (C1, C2). B) Agonist-induced secretion of α -granules (P-Selectin) and δ -granules (CD63) was evaluated by flow cytometry (FC) in diluted (PRP) from patients (back bars) and two unrelated controls (white bars). Platelets were stimulated (30 min at RT) with the indicated agonist in the presence of CD41*APC and CD62*PE or CD63*PE antibodies. Then, the samples were evaluated by FC using an Accuri C6 flow cytometer. Bars correspond to the mean, plus standard deviation, of the median fluorescence intensity (MFI) for CD62*PE (P-Selectin) and CD63*PE in the three R1213* carriers from family 18 and two unrelated controls.

Figure S6. DIAPH1 protein level in platelet lysates from R1213* carriers and unrelated healthy controls.

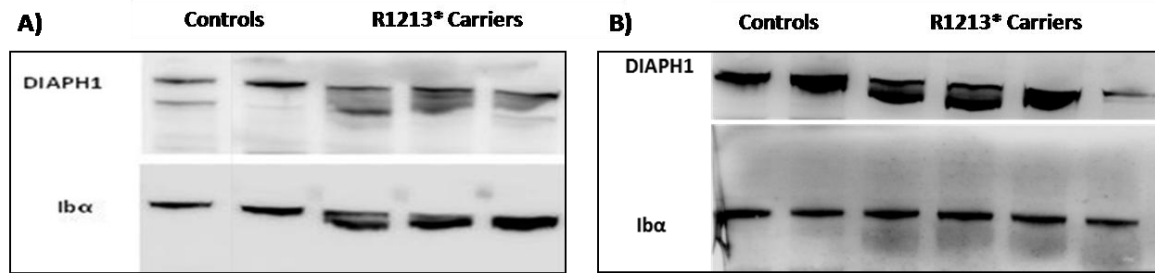


Figure S6 Legend. Washed platelets and total platelet lysates were prepared from citrated blood from carriers of the R1213* variant from pedigrees 18 and 19, and from two unrelated controls. Proteins in the lysates were separated by SDS–polyacrylamide gel electrophoresis on 4%–20% gradient gels and transferred to polyvinylidene fluoride membranes (Millipore). The total platelet content of DIAPH1 protein was assessed by standard immunoblotting, using an anti-DIAPH1 antibody (ERP7948, Abcam) previously reported,⁶ followed by an appropriate peroxidase labeled secondary antibody, and chemiluminescence detection with ECL kit (GE Healthcare). The level of GPIbα (using LJ-Ib10 anti-GPIbα antibody) was quantified as an internal control of platelet protein loading. As shown, the DIAHP1 protein is expressed in all R1213* carriers from families 18 (Panel A) and 19 (Panel B), although a mild reduction in level is apparent in most of them as compared to controls.

Figure S7. Tubulin β 1 expression pattern in platelets from a R1213* carrier and an unrelated control.

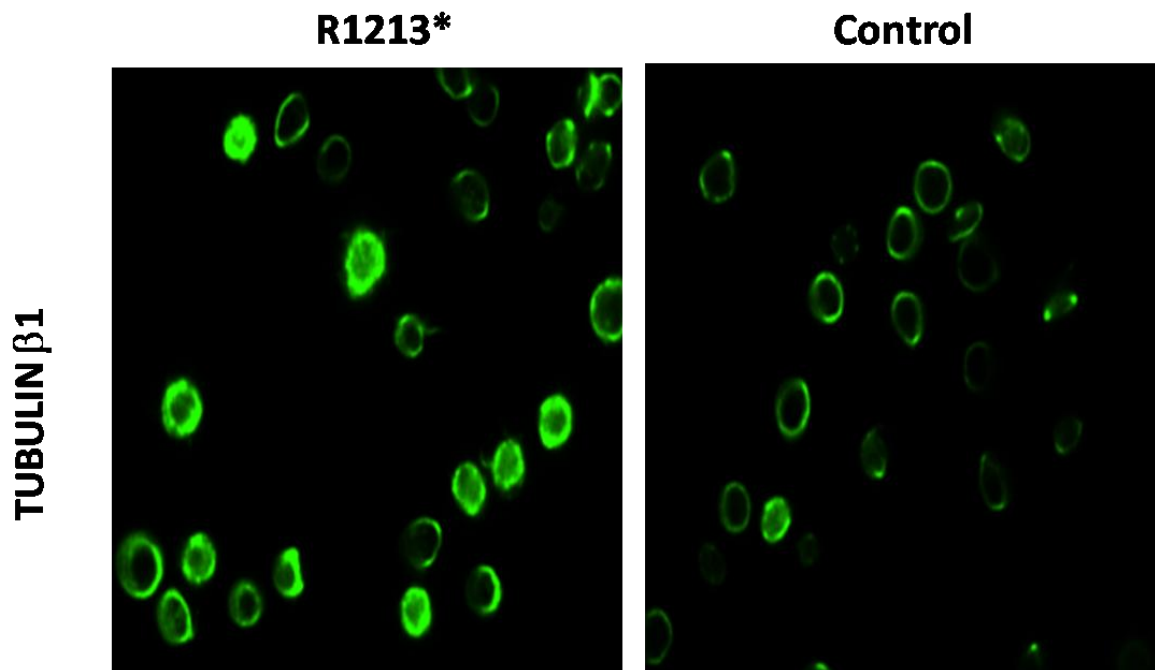


Figure S7 Legend. Detection of β 1-tubulin in platelets from the index case 18 and from an unrelated control was performed by standard immunofluorescence microscopy³. Briefly, diluted platelet-rich-plasma (20.00 platelet/uL) was placed onto(PLL)-coated slides, fixed with 4%formaldehyd, permeabilized and blocked with 4% BSA/0.1% Triton X-100 in PBS (90 min, RT). Then, cells were incubated with anti- β 1-tubulin antibody (SAB1408037, Sigma-Aldrich) (1:100 in PBS containing 0.5% BSA/0.1% Triton X-100; 90 min, RT), followed by the appropriate Alexa Fluor 546–conjugated secondary antibodies (Thermo Fisher Scientific). Fluorescence was analyzed on a Leica 6000B microscope (Leica Microsystems, Madrid, Spain). As shown, platelets from a R1213* carrier displayed higher labeling for β 1-tubulin, both in the periphery and in inside the cells.

Figure S8. Detection of the uncommon rs39428292 variant in *RBM8A* and a microdeletion in 1q21.1 in patient 30 confirmed diagnosis of TAR.

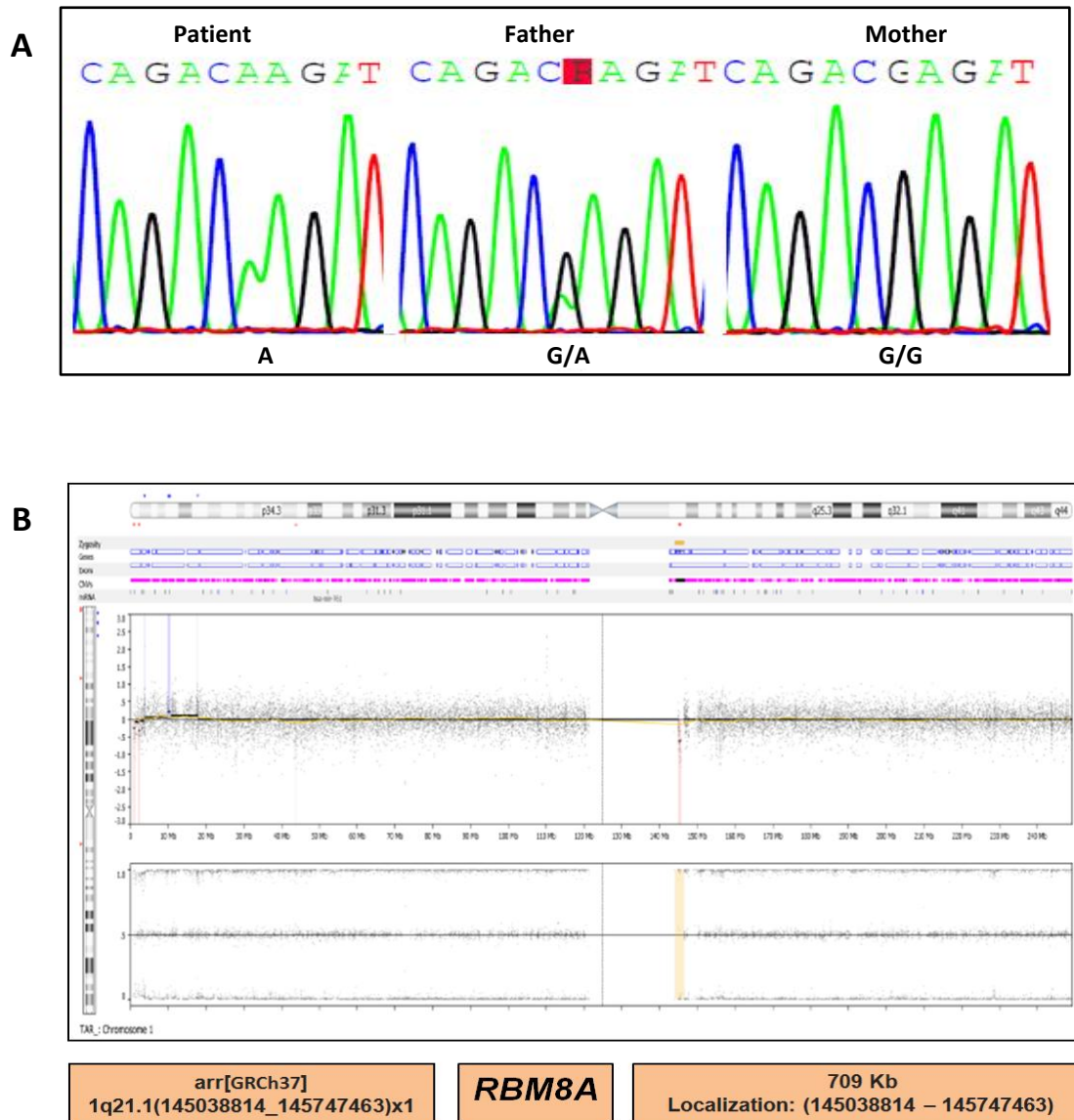


Figure S8 Legend. HTS test of DNA from case 30 identified the c.21G>A variant in *RBM8A* (rs39428292). A) Sanger sequencing confirmed the variant in hemizyosity in the patient and in heterozygosity status in his healthy father. B) CGH array analysis of patient DNA revealed a loss of heterozygosity in a 709 kb region in 1q21.1 which involved *RBM8A*.

Figure S9. Detection of 21q deletion in patient 29 by massively parallel sequencing copy number variation analysis.

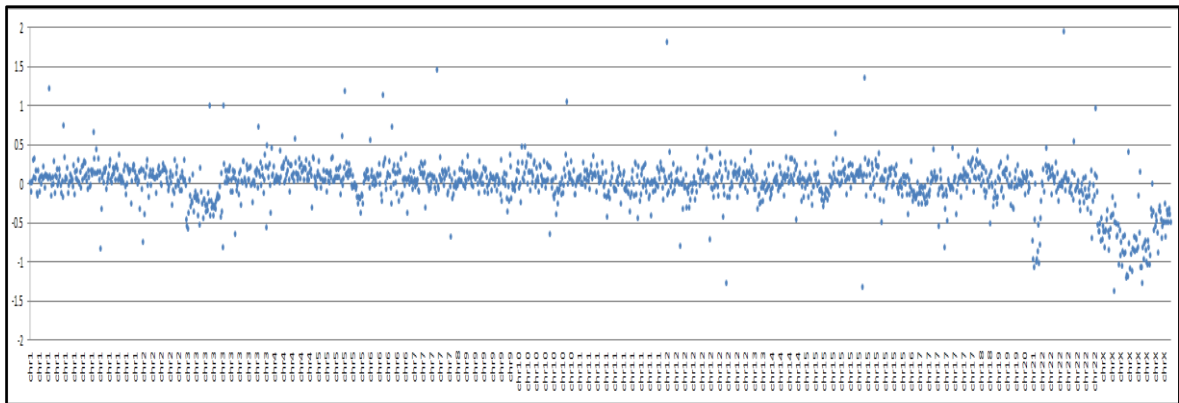


Figure S9 Legend. Whole-genome profiles of log₂ ratios of normalized mean coverage of individual exon target of a gene to that of the reference, was plotted against the target. The x-axis shows the targets in the panel plotted by relative genome order. The y-axis corresponds to the log₂ ratio of mean coverage of testing to that of reference. CNVs were called using fixed thresholds representing the minimum log₂ ratio for gains (0.40) and maximum log₂ ratio for losses (-0.55). An atypical log₂ normalized coverage ratio <0.5 suggests a heterozygous deletion of chr21 (21q region, *RUNX1*). The mean coverage depth of each individual exon target of a sample was first normalized for the total amount of the DNA template loaded onto sequencing flow cells based on the total reads of this sample. The mean coverage of each individual target from the reference samples thus obtained was used as the reference for a specific exon. Reference coverage profile for a normal sample was generated. To detect CNVs, the normalized coverage of each exon of a test sample was compared to the mean coverage of the same target in the reference file generated above⁷.

